CHEMISTRY OF MATERIALS

Article

pubs.acs.org/cm

[70]PCBM and Incompletely Separated Grades of Methanofullerenes Produce Bulk Heterojunctions with Increased Robustness for Ultra-Flexible and Stretchable Electronics

Suchol Savagatrup,[†] Daniel Rodriquez,[†] Adam D. Printz,[†] Alexander B. Sieval,[‡] Jan C. Hummelen,[‡,§] and Darren J. Lipomi*,[†]

[†]Department of NanoEngineering, University of California, San Diego, 9500 Gilman Drive, Mail Code 0448, La Jolla, California 92093-0448, United States

[‡]Solenne BV, Zernikepark 6-8, 9747 AN, Groningen, The Netherlands

[§]Stratingh Institute for Chemistry and Zernike Institute for Advanced Materials, University of Groningen, Nijenborgh 4, 9747 AG, Groningen, The Netherlands

Supporting Information

ABSTRACT: An organic solar cell based on a bulk heterojunction (BHJ) of a polymer and a methanofullerene ([60]PCBM or [70]PCBM) exhibits a complex morphology that controls both its photovoltaic and mechanical compliance (robustness, flexibility, and stretchability). Methanofullerenes are excellent electron acceptors; however, they have relatively high cost and production energy (in the purest samples) compared to other small-molecule semiconductors. Moreover, [60]PCBM and [70]PCBM—typical of van der Waals solids—can be stiff and brittle. Stiffness and brittleness may lower the yield of working modules in roll-to-roll manufacturing, shorten the lifetime against mechanical failure in outdoor conditions, and jeopardize wearable and portable applications that demand stretchability or extreme flexibility. This paper tests the hypothesis that "technical grade" PCBM (incompletely separated but otherwise pure blends containing ≥ 90% [60]PCBM or [70]PCBM) could lower the cost of manufacturing organic solar cells while simultaneously increasing their mechanical stability. Measurements of the tensile modulus of five methanofullerene samples, "technical grades" and 99% grades of both [60]PCBM and [70]PCBM, and a 1:1 mixture [60]PCBM and [70]PCBM, along with their blends with regioregular poly(3-hexylthiophene) (P3HT), lead to two important conclusions: (1) films of pure [70]PCBM are approximately five times more compliant than films of pure [60]PCBM; BHJ films with [70]PCBM are also more compliant than those with [60]PCBM. (2) BHJ films comprising technical grades of [60]PCBM and [70]PCBM are approximately two to four times more compliant than are films made using 99% grades. Tensile modulus is found to be an excellent predictor of brittleness: BHJs produced with technical grade methanofullerene accommodate strains 1.4−2.2 times greater than those produced with 99% grades. The smallest range of stretchability was found for BHJs with 99% [60]PCBM (fracture at 3.5% strain), while the greatest was found for technical grade [70]PCBM (11.5% strain). Mechanical properties are correlated to the microstructures of the blended films informed from analyses of UV−vis spectra using the weakly interacting H-aggregate model. Photovoltaic measurements show that solar cells made with technical grade [70]PCBM have similar efficiencies to those made with higher-grade material but with decreased cost and increased mechanical robustness.

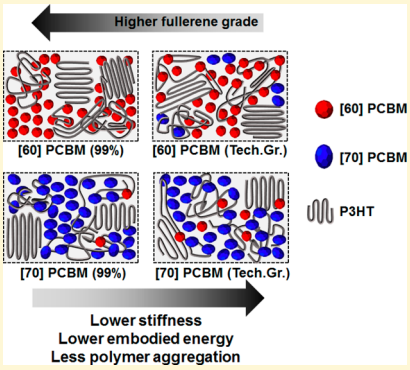

1. INTRODUCTION AND BACKGROUND

1.1. Methanofullerenes in Organic Solar Cells.

Increasing the mechanical compliance of organic semiconductors in a way that does not sacrifice electronic performance will accomplish two goals. The first goal is to improve the lifetime against mechanical failure for printed, flexible devices.[1] The second goal is to enable a new class of ultraflexible and intrinsically stretchable devices for portable, lightweight power sources,[2] wearable and implantable health monitors,[3] and fracture-proof consumer electronics.[4] One important application of organic semiconductors is the organic solar cell, in which fullerenes and their derivatives are present in all of the most efficient devices produced to date.[5] The high electron mobilities of fullerenes,[6] the solubility of methanofullerenes (e.g., [60]PCBM and [70]PCBM, Figure 1), high rates of charge transfer,[7] and their spherical (or quasi-spherical) shape, which permits transfer of an electron from any direction, suggest that fullerenes will continue to be the material of choice for a variety of applications. These materials, however, have high embodied energy in their purest form,[8,9] and polymer:-methanofullerene bulk heterojunction (BHJ) films are stiffer, more brittle, and have lower cohesive energy in comparison to

Received: February 17, 2015
Revised: May 8, 2015
Published: May 11, 2015

DOI: 10.1021/acs.chemmater.5b00638
Chem. Mater. 2015, 27, 3902−3911

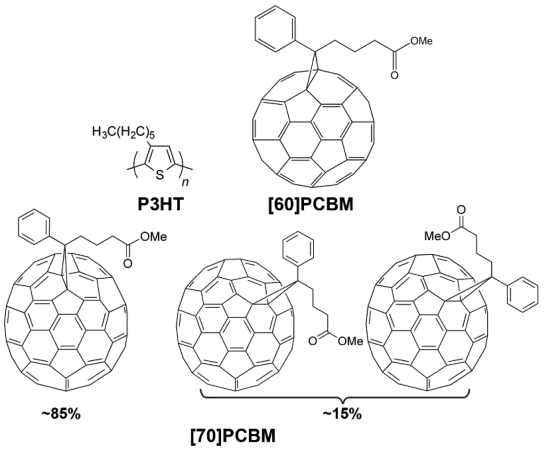

Figure 1. Chemical structures of poly(3-hexylthiophene) (P3HT) and the methanofullerenes studied. Isomers of [70]PCBM depicting the structures of the chiral α-type isomer (left) and the two possible β-type isomers (right). The α-type isomer is present in 85%, and the two β-type isomers are present in approximately equal amounts. More isomers exists in theory (not in figure), but at most in very small amounts (from HPLC and ^{1}H NMR) (see also ref 18).

films of the pure polymer.[10−12] Additionally, the high energies of production (because of the resources needed to separate them by chromatography) are correlated with the high cost of methanofullerenes (compared to conjugated polymers and small molecules, such as copper phthalocyanine).[9] We hypothesized that disorder introduced into BHJ films in the form of isomers or mixed sizes within the PCBM phases would affect the mechanical properties of polymer:methanofullerene BHJ blends, which will influence the yield of working devices during roll-to-roll coating[13] and the lifetime against mechanical failure in outdoor or portable environments, or in stretchable and ultraflexible applications.[1,14] By using "technical grades" of PCBM,[15−17] in which the C_{60} and C_{70} derivatives are incompletely separated but otherwise pure, it might be possible to address two problems at the same time: reducing the cost and production energy of organic solar cells and simultaneously increasing the mechanical resilience. While our group and others have examined the role of the polymer in determining the deformability of the active components in ultracompliant systems, the role of small molecule semiconductors—of which methanofullerenes may be the most prominent class—has not been explored.

1.2. Embodied Energy of Methanofullerenes. Fullerenes have high energies of production, in part, because they need to be separated from the carbon soot produced by the two common methods of production: pyrolysis (of toluene or tetralin) or arc plasma with graphite as a feedstock.[9] According to the analysis by Anctil et al., pyrolysis requires 146 kg of tetralin to produce 1 kg of C_{60} and 0.78 kg of C_{70}.[9] C_{70} has a greater production energy than does C_{60} largely because C_{70} is more difficult to separate from higher-order fullerenes than is C_{60}; the purification steps (from 95% to 99.9% purity) increase the embodied energy of C_{60} by a factor of two and of C_{70} by a factor of three.[9] The net result is that the embodied energies of [60]PCBM and [70]PCBM (after functionalization of the fullerene core) at 99.9% purity are 65 GJ kg^{-1} and 90 GJ kg^{-1}, respectively.[9] (While these values are nearly an order of magnitude higher than those of polysilicon,[19] methanofullerenes are present in much smaller absolute amounts in organic solar cells than polysilicon is present in conventional cells.) The contribution of methanofullerenes to the cumulative energy demand of an entire module, however, is substantial: from 19% to 31% depending on the choices of other materials in devices in which the electron donor is a polymer.[20] Substantial savings in embodied energy (which correlates well with cost for manufactured products)[9] are thus possible if one can use mixtures of methanofullerenes. The use of these mixed methanofullerene derivatives (technical grades) will produce different morphologies in BHJ films than will highly purified samples. For example, Andersson et al. showed a drastic change in the morphology of a polymer:[60]PCBM blend with the addition of <10% [70]PCBM to the methanofullerene component.[15] One expects these different morphologies to affect not only the electronic performance of the blend, but also its compliance and mechanical stability[15,21] through the effect of increased free volume in mixtures of molecules of different sizes or isomers.

1.3. Mechanical Properties and Morphology of the Bulk Heterojunction. Organic semiconductors exhibit a wide range of tensile moduli, ranging from 30 MPa to 16 GPa,[11] and propensity to fracture, from <2.5% strain to greater than 150% strain on elastic substrates.[22] This disparity suggests that modules composed of different organic semiconductors may have unequal yields during mechanically rigorous roll-to-roll manufacturing processes, unequal lifetimes in the environment, and unequal amenabilities to stretchable and ultraflexible applications.[23] One key determinant of the variation in mechanical properties in the active layer of an organic solar cell is the morphology of the donor−acceptor BHJ. Morphology refers to the details of molecular mixing, the texture and degree of crystallinity of the phases, and the extent of phase separation.[24] These key parameters have a large influence on the power conversion efficiencies of organic solar cells, given materials with good charge-transport properties, complementary absorption, and favorable relative positions of their frontier molecular orbitals. It has been shown that the mechanical properties of BHJ systems comprising conjugated polymers and small molecules are influenced by many aspects of the chemical structure (e.g., the presence of the fused or isolated rings in the main chain,[25,26] length and the composition of pendant groups,[10,27] size and intermolecular forces within crystallites)[22] and microstructural order (e.g., the addition of methanofullerene,[10,11,21,25−27] intercalation of methanofullerenes between side chains of polymers,[28,29] effect of processing conditions,[21] presence of plasticizing additives).[10,30] One aspect of the makeup of the BHJ whose effects on the mechanical properties have not been explored is the makeup (i.e., size and purity) of the methanofullerene phase.

We thus investigated two methanofullerene derivatives—[60]PCBM and [70]PCBM—at two different grades—99% grade and technical grades (≥ 90% either [60]PCBM or [70]PCBM and the remainder the other) along with their blends with regioregular poly(3-hexylthiophene) (P3HT). The hypothesis that guided our experiments was that the use of methanofullerene samples with technical grades of [60]PCBM and [70]PCBM (i.e., incomplete separation of C_{60} and C_{70} derivatives) would form BHJ films with greater compliance than films in which the methanofullerene sample was of 99% grade. We measured two mechanical properties, the tensile modulus and the ductility (as manifested in the crack on-set strain), of P3HT:methanofullerene films before thermal annealing (as-cast, AC) and after thermal

DOI: 10.1021/acs.chemmater.5b00638
Chem. Mater. 2015, 27, 3902−3911

annealing (annealed, AN) as well as pure methanofullerene films. The tensile moduli were measured using the mechanical buckling technique.[31,32] The crack-onset strains were used to measure the ductility of the film on a stretchable substrate. We observed trends in the mechanical properties that were correlated with the microstructures of the blended films informed from analyses of UV−vis spectra using the weakly interacting H-aggregate model. Our results led us to conclude that it is possible to increase the mechanical compliance of a BHJ film by using technical grade methanofullerenes (thereby lowering the cost and embodied energy), which produce statistically similar photovoltaic efficiencies.

2. RESULTS AND DISCUSSION

2.1. Mechanical Properties of Pure Methanofullerene and Bulk Heterojunction Films. We measured the tensile moduli of films using the buckling technique.[11,31] Briefly, the film of interest was spin-coated onto a passivated glass slide, then transferred to an elastomeric substrate bearing a small tensile prestrain. The prestrain was then released, and the resulting compression forced the film to adopt buckles. For the BHJ films, the tensile modulus of each film, E_f, was calculated from the measured buckling wavelength, λ_b, the thickness of the film, d_f, the tensile modulus of the substrate, E_s, and the Poisson's ratios of the film and the substrate, ν_f and ν_s, using eq 1:

$$E_f = 3E_s\left(\frac{1-\upsilon_f^2}{1-\upsilon_s^2}\right)\left(\frac{\lambda_b}{2\pi d_f}\right)^3 \quad (1)$$

However, the high stiffness and brittleness of the pure methanofullerenes caused the films to fracture when the prestrain was released; this damage precluded accurate measurements.[10,33] To avoid this problem, we performed the measurement on a bilayer system comprising a PEDOT:PSS film and the pure methanofullerene film. We chose the layer of PEDOT:PSS as the second layer to behave as a substrate with favorable surface energy and allow for a uniform film of pure methanofullerene. Studies on the interface mixing of PEDOT:PSS and the layer of P3HT:PCBM by Huang et al.[34] and Dupont et al.[35] have shown that very little methanofullerene diffuses into PEDOT:PSS at room temperature, and thus we assumed the presence of a distinct interface. We then used eq 2 to calculate the modulus of the methanofullerene film ($E_{f,2}$) (Figure 2a, dark gray bars) from the effective modulus of the bilayer (E_{eff}) and the modulus of the PEDOT:PSS film ($E_{f,1}$);[32] both E_{eff} and $E_{f,1}$ are obtained separately via the typical buckling method. (A detailed explanation of the calculation is provided in the Supporting Information.)

$$E_{eff} = \frac{1 + m^2n^4 + 2mn(2n^2 + 3n + 2)}{(1+n)^3(1+mn)}E_{f,1};$$
$$\text{where } m = \frac{E_{f,2}}{E_{f,1}},\ n = \frac{d_{f,2}}{d_{f,1}} \quad (2)$$

From the results summarized in Figure 2, panel a and Table 1, the moduli of the pure [60]PCBM films were higher than the pure [70]PCBM films for both technical grade (Tech. Gr.) and 99% samples. We attributed this observation to the greater tendency of [60]PCBM to pack efficiently and to crystallize.[36,37] The difference in behavior is consistent with the presence of isomers in [70]PCBM, which hinder efficient packing. Importantly, we observed that technical grade [60]PCBM had a lower modulus than 99% [60]PCBM. The average value for technical grade [70]PCBM was somewhat lower than for 99% [70]PCBM but within experimental error. In addition, we observed that the value of the 1:1 mixture of [60]PCBM and [70]PCBM sat between the values of the technical grades of [60]PCBM and [70]PCBM.

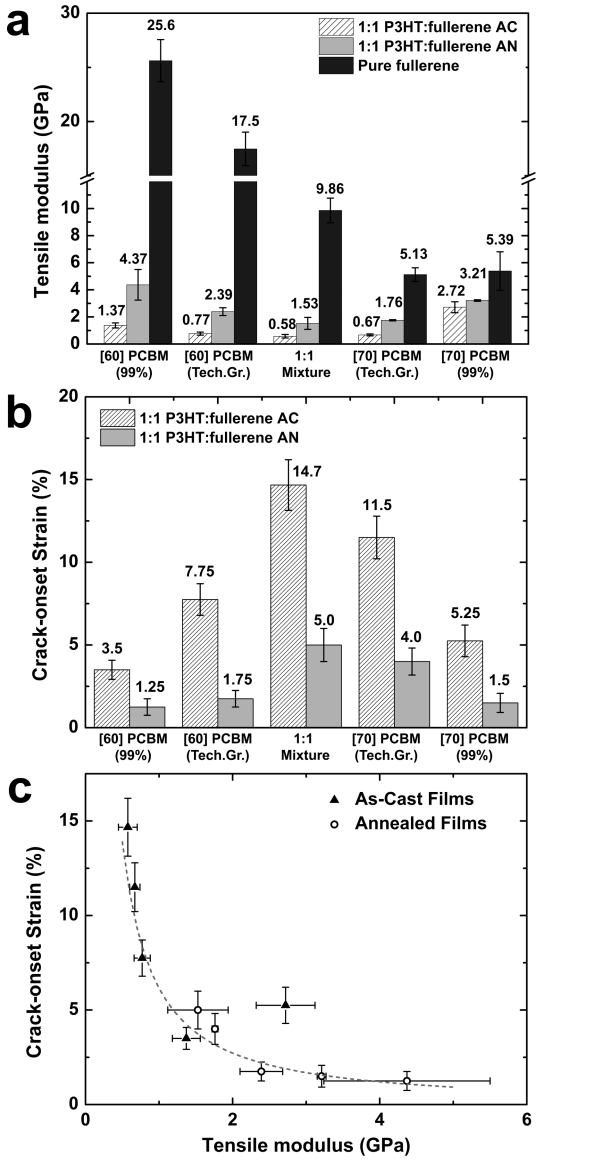

Figure 2. Mechanical properties of the BHJ and pure methanofullerene films, arranged from left to right in order of increasing content of [70]PCBM. (a) Tensile moduli of films tested in this work. The dark gray bars represent the tensile moduli of pure methanofullerene films as obtained from the bilayer method. The bilayer systems consisted of PEDOT:PSS:methanofullerene. The light gray bars and gray bars represent the moduli of blends of P3HT:methanofullerene (1:1 ratio) spin-coated from chloroform solution for both as-cast and annealed films. The value of the tensile modulus of the pure P3HT film measured in parallel to these experiments was 0.55 ± 0.09 GPa. (b) Uniaxial crack-onset strains of the thin films transferred onto PDMS substrate. All pure methanofullerene films cracked at strains below 0.5%. (c) Plot of the correlation between crack-onset strains and tensile moduli of all the films tested.

DOI: 10.1021/acs.chemmater.5b00638
Chem. Mater. 2015, 27, 3902−3911

Table 1. Summary of Tensile Moduli of the Methanofullerene Films Tested in This Work with the Buckling-Based Method and the Bilayer Technique.[a] The Value of the Pure As-Cast P3HT Used in This Experiment, Obtained in Parallel, Was 0.55 ± 0.09 GPa

	tensile modulus (GPa)				
materials	[60]PCBM (99%)	[60]PCBM (Tech. Gr.)	1:1 mixture	[70]PCBM (Tech. Gr.)	[70]PCBM (99%)
pure methanofullerene[b]	25.6 ± 1.95	17.5 ± 1.55	9.86 ± 0.91	5.13 ± 0.50	5.39 ± 1.42
P3HT:methanofullerene (1:1, as-cast)[c]	1.37 ± 0.19	0.77 ± 0.11	0.58 ± 0.13	0.67 ± 0.07	2.72 ± 0.40
P3HT:methanofullerene (1:1, annealed)[c]	4.37 ± 1.13	2.39 ± 0.29	1.53 ± 0.44	1.76 ± 0.04	3.21 ± 0.06

[a]The bilayer technique uses the buckling-based method to obtain the effective modulus of the bilayer system comprising a layer of PEDOT:PSS film (modulus obtained separately) and pure methanofullerene film and then backs out the modulus of the pure methanofullerene film. [b]Obtained from the modified bilayer technique. [c]Obtained from conventional buckling-based method.

Table 2. Summary of Crack-Onset Strains of the Thin Films When Transferred onto PDMS Substrate

	crack-onset strain (%)				
materials	[60]PCBM (99%)	[60]PCBM (Tech.Gr.)	1:1 mixture	[70]PCBM (Tech. Gr.)	[70]PCBM (99%)
pure methanofullerene	<0.5	<0.5	<0.5	<0.5	<0.5
P3HT:methanofullerene (1:1, as-cast)	3.5 ± 0.58	7.75 ± 0.98	14.7 ± 1.53	11.5 ± 1.29	5.25 ± 0.96
P3HT:methanofullerene (1:1, annealed)	1.25 ± 0.5	1.75 ± 0.5	5.0 ± 1.0	4.0 ± 0.82	1.5 ± 0.58

We then characterized the mechanical properties of the P3HT:methanofullerene blends. We used a single polymer (regioregular P3HT) to isolate the effects of the methanofullerene. We selected regioregular P3HT because it is the most widely studied material in the literature for BHJ OPV devices.[38] While it has not produced state-of-the-art values of *PCE* in several years[39] (though some recent reports have been favorable),[40] it seems to be especially amenable to scale-up by roll-to-roll coating[41] because it works well in relatively thick films, and it has a low cost due to its short synthetic route.[8,42] Moreoever, the morphology of P3HT when mixed with [60]PCBM is the basis for many studies in the field,[38] and the mechanical properties of pure P3HT and P3HT:[60]PCBM films have been well characterized.[10,11,21,25] In previous publications by our group, we reported the tensile modulus of pure P3HT to be 1.09 ± 0.15 GPa.[10] This value was in the range of those reported by various groups, or 0.22−1.33 GPa.[11,21,25] The modulus of the batch of pure P3HT used in this study was 0.55 ± 0.09 GPa, approximately half the value we obtained in our previous study.[10] We attribute the differences in moduli commonly obtained for P3HT (and generally not other materials) primarily to the closeness of its glass transition temperature (T_g = 12−25 °C)[43,44] to ambient temperature, and possibly to the sensitivity of its T_g to batch-to-batch variability. Our principal concern, however, was not with the absolute values of the tensile moduli but with the effects of the methanofullerene component.

Figure 2, panel a shows the tensile modulus of the BHJ films, and Table 1 summarizes the tensile moduli of the films tested in this work. The crack-onset strains (Figure 2b, Table 2) correlate well with the measured tensile moduli: films with higher moduli are more brittle (Figure 2c). While we note that the crack-onset strains provide a measurement of the apparent brittleness of the active layer films, the mechanical properties of complete solar cell devices will be dependent not only on the P3HT:methanofullerene active layer, but also on all other components of the device (e.g., the substrate and the electrode). However, in the case that the substrate and the electrode are more compliant than the active layer,[30] the active layer will be the limiting factor in the mechanical compliance and robustness of solar cell devices. In stretchable devices for wearable or biologically integrated applications, all components must accommodate tensile strain in a specified range.

The data in Figure 2 reveal four salient features: (1) all BHJ films were stiffer than films of the pure polymer (consistent with previous results[10,11,21,25]); (2) thermal annealing increased the stiffness of all BHJ films;[22,27] (3) technical grade methanofullerenes and 1:1 mixture of [60]PCBM and [70]PCBM produced lower moduli in the BHJ films; (4) films containing principally [70]PCBM were more compliant than films containing principally [60]PCBM given the same thermal history in three of four cases. The following discussion attempts to explain these key observations using spectroscopic and photovoltaic measurements and arguments from the literature.

2.2. Stiffening Effect of Methanofullerenes on the Pure Polymers. The current model of the BHJ, which has been derived principally from blends of P3AT and [60]PCBM, comprises a three-phase system: an aggregated polymer-rich phase, a methanofullerene-rich phase, and a well-mixed amorphous phase.[38] The mixed phase forms as a consequence of the miscibility of methanofullerene molecules within the amorphous domains of the polymer,[45,46] and thus the current model predicts the absence of pure amorphous polymer domains in P3HT:PCBM films. In a compelling visualization of the evolution in morphology of the BHJ, Roehling et al. used electron-tomographic three-dimensional reconstructions of a blend before and after annealing (using an endohedral methanofullerene for phase contrast) and showed a clear reduction of the fraction of the mixed phase.[47] The ratio of phases within the ternary system went from (P3HT:methanofullerene:mixed) 28:28:44 (as-cast) to 50:37:13 (annealed), or "mostly mixed" to "mostly crystalline P3HT".[47]

The crystalline phases of methanofullerenes have been characterized in detail.[48] In particular, Zheng et al. observed a striking evolution in crystalline morphology in pure [60]PCBM films from needle-like, to axialite, to faceted crystalline slices.[49] A similar transformation was observed in crystallites grown in the interface between a solvent and a nonsolvent.[50] In blended films of P3HT:[60]PCBM, Verploegen et al. used grazing incidence X-ray scattering (GIXS) to measure the evolution in crystallization of the two components during thermal annealing and observed diffraction peaks consistent with crystalline

DOI: 10.1021/acs.chemmater.5b00638
Chem. Mater. 2015, 27, 3902−3911

[60]PCBM.[36] Indeed, [60]PCBM is known to form crystals upon extended annealing that are large enough to be visible by optical microscopy.[51] Thus, the current model predicts that the [60]PCBM-enriched phase in the BHJ is at least partially crystalline.[38] Because of the presence of isomers in [70]PCBM, however, it has not been observed to crystallize in neat films or in blends. The disorder in [70]PCBM was the basis of our hypothesis that the larger methanofullerene might produce films with reduced stiffness.

In every instance in which the moduli of pure conjugated polymers and their blends with fullerenes are reported in the same paper, the blends are stiffer than the pure polymer.[10,11,21] The mechanical properties of pure P3ATs are influenced, among other factors, by the degree of crystallinity and the T_g of the amorphous domains relative to ambient temperature. The proximity of T_g to ambient temperature suggests that the temperature at which experiments are carried out is near the high end of the range in which P3HT is in the glassy state. While the ordered domains of P3HT are generally unaffected by the presence of methanofullerenes in BHJ films,[52] the pure amorphous phase of the polymer is consumed by methanofullerene to form the mixed phase. Methanofullerene molecules not dispersed in the mixed phase form a third, methanofullerene-enriched phase that is either amorphous or partially ordered (in the case of [60]PCBM, which can pack efficiently because it is a single isomer). Differences in mechanical properties between the pure polymer and the BHJ can thus be attributed to the effects of the mixed phase and the methanofullerene-enriched phase. Because the pure methanofullerene films are stiffer than either pure P3HT or the corresponding BHJ, we predicted that the methanofullerene-enriched domains behave as stiff inclusions within the BHJ film. We also suspect that the mixed phase in a BHJ film is stiffer than the amorphous phase in pure P3HT. This behavior is consistent with the observation by Hopkinson et al., and confirmed by us, that the addition of [60]PCBM increases T_g of P3HT, that is, [60]PCBM is an antiplasticizer.[53] The high modulus of the P3HT:[60]PCBM blend relative to the pure polymer is also predicted on the basis of the composite theory applied to BHJ films by Tahk et al.,[11] but the agreement may be serendipitous because it does not take into account the presence of pure, unmixed phases. In a separate study, our group has shown that the ratio of the polymer to methanofullerene also strongly influenced the mechanical properties of the resulting BHJ films; the tensile modulus increased when the weight percentage of methanofullerene was increased from 0% to 50%.[54]

2.3. Stiffening Effect of Thermal Annealing. A trade-off between electronic and mechanical properties has been observed in the context of thermal history of organic semiconductors.[21] Generally, postprocessing treatment such as thermal annealing increases the crystallinity of the materials, which usually improves the electrical properties but in some cases increases the stiffness. For example, films of PBTTT doubled in tensile modulus after thermal annealing,[22] while pure P3HT films exhibited a minimal change in modulus.[21,25] The effect of thermal annealing of pure polymer films on the mechanical properties is thus not generalizable. Polymer:methanofullerene blends, however, have been consistently shown to increase in tensile modulus with thermal treatment.[27] The origin of the increase in modulus is the thermally evolved microstructure of the ternary blend. As-cast P3HT:PCBM films are characterized by low order and a large percentage of mixed phase.

An increasing volume fraction of ordered polymer and methanofullerene-enriched phases should be correlated with an increase in modulus of the blended film. Order in P3HT can be determined using a widely practiced method based on the work of Spano and co-workers, who showed that the UV−vis spectra of the polymer can be deconvoluted into contributions from the aggregated (i.e., ordered) and amorphous phases utilizing the weakly interacting H-aggregate model.[55] The ratio of these contributions, after taking into account the unequal absorption coefficients of the ordered and the amorphous domains, can be used to determine the percent aggregated polymer. To analyze the order of different P3HT:methanofullerene blends, we first obtained the UV−vis spectra of the blend and then subtracted the absorption of the pure methanofullerene. Figure 3, panels a and b show the evolution in the UV−vis spectra of the P3HT component of the P3HT:methanofullerene blends. The absorption due to the methanofullerenes was approximated as the absorption of thin films of the methanofullerenes (prepared in the same manner as the blends) and subtracted from the spectra of the blends.[21,56] (Before subtraction, the methanofullerene absorption spectra were normalized to the peaks at 335 nm for [60]PCBM and 379 nm for [70]PCBM.) Though this method of subtraction overestimates the methanofullerene contribution to the absorption spectra, it has a minimal effect on the strongly absorbing regions of P3HT. (While we note that [70]PCBM is more strongly absorbing in the visible region than [60]PCBM, the absorbance is still dominated by the P3HT component of the blend in the visible region.) The absence of vibronic peaks (longer-wavelength shoulders) in the

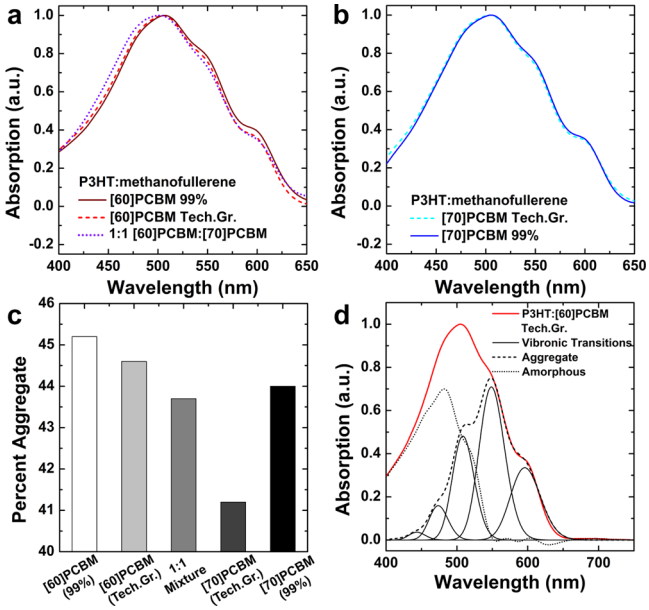

Figure 3. Absorption of P3HT:methanofullerene thin films after annealing treatment with the methanofullerene signal subtracted. (a) P3HT with [60]PCBM for 99% grade and technical grade (Tech. Gr.) along with the 1:1 mixture of [60]PCBM and [70]PCBM. (b) P3HT with [70]PCBM for Tech. Gr. and 99% grade. (c) Percent aggregate of the P3HT:methanofullerene films as calculated via the weakly interacting H-aggregate analysis. (d) Example of deconvolution of the absorption spectra using the weakly interacting H-aggregate analysis.

DOI: 10.1021/acs.chemmater.5b00638
Chem. Mater. 2015, 27, 3902−3911

as-cast films suggests the low concentration of ordered aggregates of pure polymer. A clear increase in order upon thermal annealing is observed from the differences in the UV−vis spectra. To obtain the percent of the polymer in the aggregated phase of the annealed films, we used a MATLAB program to perform a least-squares fit of the weakly interacting H-aggregate model to the experimental data. This method was introduced by Clark et al. and later used by Awartani et al. to correlate microstructure to mechanical properties,[21,57] and it produces consistent fits that are relatively insensitive to the range of bounds for the fit (as long as it is performed in the strongly absorbing region for aggregated polymer).[56] The morphology as assayed by UV−vis was not dependent on the substrate: spin-coating the BHJ films on glass treated with oxygen plasma, passivated with a fluorinated silane monolayer, or on glass bearing a film of PEDOT:PSS produced indistinguishable UV−vis spectra (Figure S1, Supporting Information).

2.4. Effect of Incomplete Separation of [60]PCBM and [70]PCBM in Technical Grades. Enrichment of [60]PCBM and [70]PCBM from technical grade to 99% increased the tensile modulus of the resulting films. We attributed this effect to two factors. The first factor is that neat films of the technical grade methanofullerenes had lower tensile moduli (though the moduli of neat films of technical grade [70]PCBM and 99% [70]PCBM were within error, those of the corresponding BHJ films were not). If the packing structures of the methanofullerene-enriched phases in the BHJ films resemble those of the neat methanofullerene films, then it stands to reason that the stiffening effect of the methanofullerene-rich inclusions would be reduced for technical grade samples in the BHJ films. One possible reason for decreased stiffness of the technical grade samples may be a consequence of less efficient packing of methanofullerenes in the presence of molecules of the "wrong" size. There may be a differential stiffening effect between [60]PCBM and [70]PCBM on the mixed phase of the BHJ, which may account for the fact that the moduli of the BHJ comprising technical grade [70]PCBM were less stiff than the one comprising 99% [70]PCBM, even though the moduli of the neat [70]PCBM films of both grades were similar. We admit to some uncertainty in rationalizing the greater modulus (though also greater ductility) of the as-cast P3HT:methanofullerene blend comprising 99% [70]PCBM compared to that of the as-cast blend comprising 99% [60]PCBM, especially in light of the significantly lower modulus of unblended 99% [70]PCBM compared to 99% [60]PCBM. We note, however, that the mechanical properties will not necessarily be proportional to the modulus of the pure methanofullerene component because differences observed between blended films comprising [60] and [70]PCBM are dependent on at least four factors: (1) unequal miscibility of [60]PCBM and [70]PCBM in amorphous P3HT; (2) unequal antiplasticization even given the same miscibility; (3) unequal influence on the aggregation behavior of the polymer; and (4) packing structures—and thus mechanical properties—within the methanofullerene-enriched phases that do not necessarily resemble those in the neat methanofullerene films. Ultimately, the expected behavior was recovered upon annealing. That is, the annealed blend comprising 99% [70]PCBM had a lower modulus and greater ductility than the annealed blend comprising 99% [60]PCBM.

Another factor that may account for increased modulus of the BHJ film for 99% grade methanofullerenes is the increase in the order within the polymer phase induced by the higher-grade methanofullerene. Analysis of the spectra shown in Figure 3, panels a and b by the weakly interacting H-aggregate model[21,27,55] reveal that the percent aggregate of the polymer increases from 44.6% to 45.2% (for technical grade [60]PCBM to 99% [60]PCBM) and from 41.2% to 44.0% (for [70]PCBM technical grade to [70]PCBM 99%) (Figure 3c). The reason that the ordered polymer phase increased with increasing purity of the methanofullerene is not immediately clear. We tentatively assigned this effect, nevertheless, to the expectation that efficient packing of methanofullerene-enriched phases might remove methanofullerenes from the mixed phase and thus permit additional polymer chains to form aggregates, which are correlated with stiffer films.

2.5. Effect of Methanofullerene Size and Isomerism. Increasing the size of the fullerene core, from [60]PCBM to [70]PCBM, decreased the tensile moduli of the resulting blended films. While holding the grade and the post-treatment of the film constant, the moduli of the P3HT:methanofullerene films were lower in [70]PCBM samples compared to [60]PCBM samples (with one exception out of four pairs, the as-cast BHJ film made with 99% grade [60]PCBM was more compliant than the as-cast BHJ film made with 99% grade [70]PCBM, though the relationship was reversed after annealing). We attributed the lower compliance of BHJs comprising [70]PCBM compared to [60]PCBM principally to the presence of isomers of [70]PCBM, which impede crystallization. As shown in Figure 1, [70]PCBM exists as isomers because C_{70} has D5 symmetry.

2.6. Photovoltaic Properties. We then measured the photovoltaic properties of the four BHJ blends for which we obtained mechanical data. We fabricated the devices by mixing the methanofullerenes in a 1:1 ratio with P3HT using *o*-dichlorobenzene (ODCB) as the solvent. Given our ultimate interest in systems in which every component is stretchable, we chose PEDOT:PSS, doped with DMSO and Zonyl,[27] as the transparent anode, and eutectic gallium−indium (EGaIn) as the cathode. Figure 4, panel a shows the current density versus voltage (J−V) plots, and Table 3 summarizes the figures of merit. We observed increases in the short-circuit current (J_{sc}) in devices comprising [70]PCBM when compared to those with [60]PCBM. The observation agreed well with previously published results.[15−17] The effect of purity on J_{sc} and V_{oc} between the same methanofullerene size was minimal—similar values were obtained from [60]PCBM with technical grade and

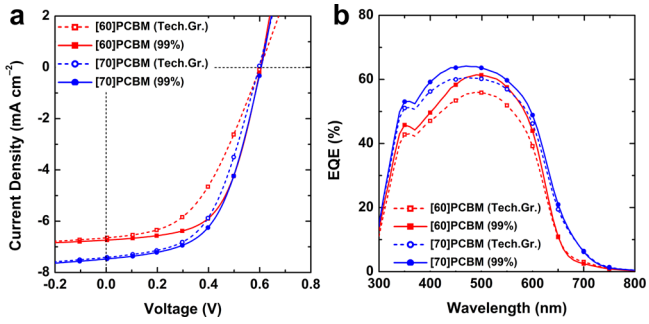

Figure 4. (a) Photovoltaic characteristic of averaged devices ($N \geq 8$) with an active layer of 1:1 blend of P3HT and respective methanofullerenes. The architecture of the devices was PEDOT:PSS/P3HT:methanofullerene/EGaIn. (b) External quantum efficiencies of the devices with the same composition.

DOI: 10.1021/acs.chemmater.5b00638
Chem. Mater. 2015, 27, 3902−3911

Table 3. Summary of the Photovoltaic Figures of Merit for P3HT:Methanofullerene Solar Cells Fabricated in This Work (N ≥ 8)[a]

device	V_{OC} (mV)	J_{SC} (mA cm^{-2})	*FF* (%)	*PCE* (%)	J_{SC}, calc from *EQE* (mA cm^{-2})
P3HT:[60]PCBM (99%)	602 ± 5.5	6.74 ± 0.2	59 ± 3.0	2.36 ± 0.2	8.27
P3HT:[60]PCBM (Tech.Gr.)	602 ± 3.7	6.60 ± 0.4	48 ± 4.8	1.89 ± 0.2	7.58
P3HT:[70]PCBM (Tech.Gr.)	598 ± 11.2	7.41 ± 0.3	53 ± 1.7	2.35 ± 0.1	8.92
P3HT:[70]PCBM (99%)	606 ± 7.5	7.47 ± 0.4	55 ± 1.3	2.48 ± 0.1	9.40

[a]The solar cell device architecture was PEDOT:PSS/P3HT:methanofullerene/EGaIn. PEDOT:PSS, doped with 7% DMSO and 0.1% Zonyl, was spin-coated to create a layer of ∼150 nm thick. The active layer was spin-coated from a solution of 1:1 P3HT:methanofullerene in ODCB (40 mg mL^{-1}) and thermally annealed at 125 °C in an inert atmosphere. EGaIn droplets were extruded to create the active area of ∼0.02 cm^{-2}.

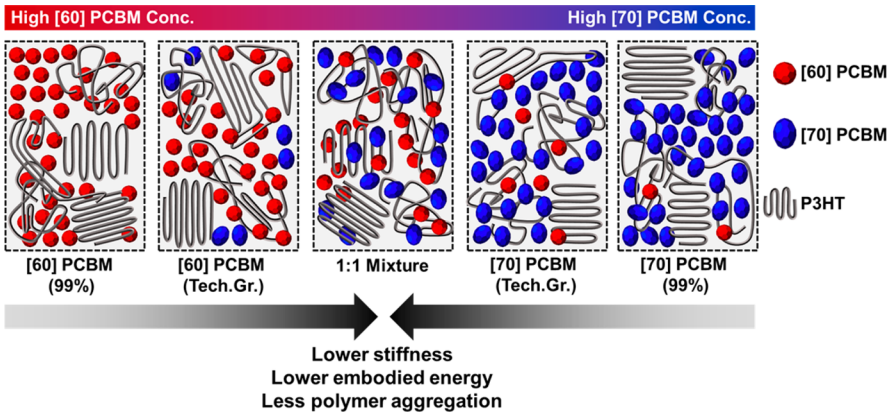

Figure 5. Schematic summary of the effect of mixed grades of methanofullerenes on the mechanical properties of P3HT:methanofullerene blends.

99% grade as well as [70]PCBM with technical grade and 99% grade. However, in this study, the 99% [60]PCBM produced an increase in the fill factor (*FF*) and therefore the power conversion efficiency (*PCE*), compared to technical grade [60]PCBM. The difference in performance between technical grade [70]PCBM and 99% [70]PCBM was within experimental error. The only methanofullerene sample of the four measured with statistically lower *PCE* than the other three was technical grade [60]PCBM.

External quantum efficiency (*EQE*) of the devices are shown in Figure 4, panel b. The effect of the size of the methanofullerenes was observed to be similar to that on the J_{sc}. High *EQE* values were observed in devices prepared from both technical grade and 99% [70]PCBM, which suggests that the photon−electron conversion processes are efficient. The purity of the methanofullerene increased the *EQE* values slightly; however, the trend in the *EQE* values generally corresponded with the *PCE* values obtained in the solar cells. We calculated the expected short-circuit current ($J_{SC,Calc}$), shown in Table 3, using the following equation:

$$J_{SC,Calc} = \int eEQE(\lambda)N_p(\lambda)\,d\lambda \quad (3)$$

Where e is the elemental charge, λ is the wavelength, $EQE(\lambda)$ is external quantum efficiency, and $N_p(\lambda)$ is the total number of incident photons per second per square centimeter, obtained from the reference solar spectral irradiance AM 1.5G. The differences in the calculated J_{SC} between technical grade and higher purity samples were small, 8% for [60]PCBM and 5% for [70]PCBM. We also observed that our measured J_{SC} values are lower than the calculated values, though within the 20% error margins outlined by Zimmermann et al.[58]

3. CONCLUSION

Organic solar cells are in principal capable of producing substantial amounts of renewable energy at low cost, but only if they can be made in high yield using techniques for high-speed (e.g., roll-to-roll) manufacturing. Furthermore, organic solar cells have the potential to occupy niches in ultraflexible, stretchable, wearable, collapsible, and portable applications, which would not be amenable to conventional—or even other thin-film—technologies. Mechanical compliance is often assumed for organic optoelectronic devices because of the ability to bend thin films to small radii of curvature. The mechanical properties, however, are not favorable for every organic semiconductor; it is important to understand these properties to mitigate potential routes of mechanical failure during fabrication and use in the outdoor environment (due to the forces of thermal expansion, wind, and precipitation, for example) and to enable stretchable and ultraflexible applications. All applications demanding moderate to extreme mechanical deformation, however, require elucidation of the interplay between molecular structure and microstructure, and their influence on the mechanical properties of organic semiconductors.

This paper explored the effect of the size and the extent of mixing of two ubiquitous methanofullerene materials on the mechanical properties of organic solar cells. Our analysis, summarized in Figure 5, illustrates the effect of the extent of mixing on the mechanical properties of polymer:methanofullerene BHJ blends. In particular, use of technical grade [70]PCBM instead of 99% [60]PCBM increased the stretchability by a factor of three (from a crack-onset strain of 3.5% to 11.5%). This increase in compliance would, for example, substantially increase the range of tensile strains available in a wearable or portable device. The influence on flexibility is also significant: the less compliant film on the surface of a substrate with a

DOI: 10.1021/acs.chemmater.5b00638
Chem. Mater. 2015, 27, 3902−3911

thickness of 200 μm could be wrapped around a cylinder with a diameter of approximately 6 mm without fracture, while the more compliant film could be wrapped around a cylinder with a diameter of approximately 2 mm. Increased deformability should also increase the lifetime against damage during repeated loading.

While an earlier study found no statistically significant influence of the ratio between [60]PCBM and [70]PCBM of several methanofullerene derivatives on the power conversion efficiency of the P3HT:methanofullerene OPV devices,[15−17] the photovoltaic measurements in this study suggest that devices made using [70]PCBM of lower grade may be slightly but not substantially less efficient than those made using materials of higher grade. We note, however, in contrast to earlier studies, that we used ITO-free anodes and EGaIn cathodes because of our underlying interest in stretchable and ultraflexible applications. These substitutions could in principle lead to small differences observed between this study and earlier ones. Lowered efficiency could be tolerated if counterbalanced by decreased cost and increased yield and lifetime.

4. EXPERIMENTAL METHODS

4.1. Materials. Methanofullerene derivatives were synthesized by Solenne BV, Groningen, The Netherlands. We conducted our experiments using five different methanofullerene samples: [60]PCBM (99% and technical grade, which was 90% [60]PCBM with the remainder [70]PCBM), and [70]PCBM (99% and technical grade, which was 93.5% [70]PCBM with the remainder [60]PCBM). Mixtures with a 1:1 ratio were prepared by mixing 99% grades of [60]PCBM and [70]PCBM by weight. Regioregular P3HT (M_n = 44 kDa, PDI = 2.0) was purchased from Sigma-Aldrich and used as received. PDMS, Sylgard 184, Dow Corning, was prepared according to the manufacturer's instruction at a ratio of 10:1 (base:cross-linker) and cured at room temperature for 36−48 h when it was used for buckling experiments. (Tridecafluoro-1,1,2,2-tetrahydrooctyl)-1-trichlorosilane (FOTS) was obtained from Gelest. PEDOT:PSS (Clevios PH1000) was purchased from Heraeus. DMSO was purchased from BDH with purity of 99.9%. Zonyl (FS-300) fluorosurfactant, chloroform, ODCB, acetone, isopropanol, and EGaIn were purchased from Alfa Aesar.

4.2. Preparation of Films. For the buckling-based method and crack-onset experiments, hydrophobic glass slides were prepared as the initial substrate for the thin films. Glass slides (2.5 cm × 2.5 cm) were cleaned by bath sonication in detergent, deionized water, acetone, and isopropanol for 15 min each and dried under a stream of compressed air. The surface was then activated with an air plasma (30 W, 200 mTorr, 3 min) before enclosing in a vacuum desiccator with FOTS. The desiccator was left under dynamic vacuum for 12 h. The glass slides were rinsed with deionized water and isopropanol and dried under a stream of compressed air before use. For buckling-based method, P3HT:methanofullerene films were spin-coated onto FOTS treated glass slides using three different spin speeds to achieve three thicknesses. For the crack-onset experiments, all films were spin-coated at the parameters to obtain similar thicknesses. The AC films were then placed under vacuum for 1 h to remove any residual solvent. The AN films were placed on the hot plate under inert atmosphere at 125 °C for 30 min before use. The films were spin-coated on plasma cleaned glass slides for UV−vis absorption experiments. We observed minimal differences in the UV−vis absorption when the films were spin-coated onto plasma-treated, FOTS-treated, and PEDOT:PSS glass slides (Figure S1, Supporting Information).

4.3. Buckling-Based Methodology and Crack-Onset Experiment. The elastomer poly(dimethylsiloxane) (PDMS) was chosen as the substrate for all mechanical measurements. The mixed and degassed prepolymer was allowed to cure at room temperature for 36−48 h before it was used in an experiment. The PDMS was then cut into rectangular pieces (l = 8 cm, w = 1 cm, h = 0.3 cm) and stretched to strains of 2% using a computer-controlled stage, which applied strain to samples using a linear actuator. While the PDMS rectangles were under strain, microscope slides (5 cm × 2.5 cm activated using oxygen plasma and treated with FOTS to later facilitate separation of the PDMS) were clipped onto the back of each rectangle using binder clips to maintain the strain. Transferring the P3HT:methanofullerene films to the prestrained PDMS substrate was performed by initially scoring the films along the edges with a razor and placing the films against the PDMS. After a minimum amount of pressure was applied to create a conformal seal between the PDMS and the P3HT:methanofullerene films, we separated the glass/stretched PDMS from the glass/conjugated polymer film in one fast motion. In most cases, the areas in which the films were in contact with the PDMS were successfully transferred to the prestrained PDMS rectangles. The binder clips were then removed, and the PDMS was allowed to relax to the equilibrium length. Buckles formed in the P3HT:methanofullerene films upon relaxation of the PDMS. Buckling wavelengths were obtained from the optical micrographs. Because of the inherent brittleness of the pure methanofullerene films, we employed the bilayer technique to obtain the tensile moduli. In these sets of experiments, a layer of PEDOT:PSS film of known tensile modulus is used as an interfacial layer. The PEDOT:PSS films were spin-coated onto the FOTS glass slides before spin-coating the pure methanofullerene films. The PEDOT:PSS layer assisted in modifying the surface energy such that the methanofullerene solutions can be easily deposited and facilitate the buckling-based experiment by lowering the effective modulus of the bilayer system. From the known modulus of the PEDOT:PSS and the measured thickness ratio between the PEDOT:PSS and the methanofullerene layer, the modulus of the methanofullerene layers was calculated using eq 2.

For crack-onset experiments, the PDMS substrates were cut into rectangular pieces (l = 8 cm, w = 1 cm, h = 0.15 cm). The P3HT:methanofullerene films were transferred onto the PDMS substrates baring no prestrain in the same manner as described above. The P3HT:methanofullerene films/PDMS was then subjected to incremental increase in uniaxial strain with a step size of 0.5%. At each step, an optical micrograph was taken and the strain at which the first crack formed was recorded.

4.4. Fabrication of Organic Solar Cells. We deposited a layer of PEDOT:PSS from an aqueous solution containing 92.9 wt % Clevios PH 1000 (~0.9−1.2 wt % PEDOT:PSS), 7.0 wt % DMSO, and 0.1 wt % Zonyl fluorosurfactant on plasma treated glass slides as the transparent anode. The solution was filtered and spin-coated at a speed of 500 rpm for 120 s, followed by 2000 rpm for 30 s. The films were then dried at 150 °C for 30 min. The photoactive layers were subsequently spin-coated on the PEDOT:PSS layer at a speed of 500 rpm for 240 s, followed by 2000 rpm for 60 s. A thin strip of the PEDOT:PSS anode was exposed by wiping away a section of the photoactive layer with chloroform for electrical contact. The samples were then immediately placed in a nitrogen-filled glovebox and annealed at 125 °C for 30 min. EGaIn was used as the top contact.

4.5. Characterization of Films. The photovoltaic properties were measured in a nitrogen-filled glovebox using a solar simulator with a 100 mW cm^{-2} flux under AM 1.5G condition (ABET Technologies 11016-U up-facing using calibrated with a reference cell with a KG5 filter). The current density versus voltage was measured using a Keithley 2400 SourceMeter. The absorbance of the materials was measured using a PerkinElmer Lambda 1050 UV−vis/NIR spectrophotometer. The wavelength range measured was 300−850 nm with a step size of 1 nm. The films were prepared in the same manner as described in the above section of preparation of films. *EQE* measurement were measured in air. The photocurrent as a function of wavelength was recorded by a multifunction optical power meter (Newport Model 2936-R) using 300 W xenon lamp and Cornerstone monochromator (Newport Model 74004) illumination.

4.6. Weakly Interacting H-Aggregate Model. In the aggregated state (i.e., crystallites in solid films), the coupled electron−vibrational (vibronic) transitions determine the absorption of weakly interactive H-aggregates and can be modeled as Gaussian fits by[21,55−57]

DOI: 10.1021/acs.chemmater.5b00638
Chem. Mater. 2015, 27, 3902−3911

$$A(E) \propto \sum_{m=0} \left(\frac{S^m}{m!}\right) \times \left(1 - \frac{W e^{-S}}{2E_p} \sum_{n \neq m} \frac{S^n}{n!(n-m)}\right)^2 \times \exp\left(\frac{-\left(E - E_{00} - mE_p - \frac{1}{2}WS^m e^{-S}\right)^2}{2\sigma^2}\right) \quad (4)$$

In eq 4, A is the absorption by an aggregate as a function of the photon energy (E). E_{00} is the energy of the $0 \rightarrow 0$ vibronic transition, which is allowed assuming some disorder in the aggregates.[55] S is the Huang–Rhys factor, which is calculated from absorption and emission spectra, and is set to 1 for P3HTs.[55,57] E_p is the intermolecular vibration energy, which (in the case where $S = 1$) is set to 0.179 eV as determined by Raman spectroscopy.[59] W is the free exciton bandwidth, which is related to the nearest neighbor interchain excitonic coupling. Upon coupling, a dispersion of the energies occurs, the width of which is equal to W (which is four times the nearest neighbor coupling). The terms m and n are the ground- and excited-state vibrational levels, and σ is the Gaussian line width. The Gaussian line width, σ, E_p, W, and the scaling factor for the calculated absorption were found by a least-squares fit to the experimental absorption in the region of 1.93–2.25 eV.[21,56,60] This region was selected because the absorption is dominated by the polymer aggregates. Above 2.30 eV, the amorphous polymer dominates absorption.[57,60]

■ ASSOCIATED CONTENT

Supporting Information

UV–vis absorption of P3HT:methanofullerene films on different substrates, photovoltaic characteristics of P3HT:methanofullerenes with 1:1 mixture of [60]PCBM and [70]PCBM, and detailed procedures for stiffness measurement via the buckling method. The Supporting Information is available free of charge on the ACS Publications website at DOI: 10.1021/acs.chemmater.5b00638.

■ AUTHOR INFORMATION

Corresponding Author

*E-mail: dlipomi@ucsd.edu.

Notes

The authors declare the following competing financial interest(s): Solenne BV produced the methanofullerene samples used in this study.

■ ACKNOWLEDGMENTS

This work was supported by the Air Force Office of Scientific Research (AFOSR) Young Investigator Program, Grant No. FA9550-13-1-0156. Additional support was provided by the laboratory startup funds from the University of California, San Diego (UCSD). S.S. acknowledges support provided by the National Science Foundation Graduate Research Fellowship under Grant No. DGE-1144086. D.R. acknowledges support from the Initiative for Maximizing Student Development at UCSD.

■ REFERENCES

(1) Savagatrup, S.; Printz, A. D.; O'Connor, T. F.; Zaretski, A. V.; Rodriquez, D.; Sawyer, E. J.; Rajan, K. M.; Acosta, R. I.; Root, S. E.; Lipomi, D. J. Mechanical Degradation and Stability of Organic Solar Cells: Molecular and Microstructural Determinants. *Energy Environ. Sci.* **2015**, *8*, 55.

(2) Kaltenbrunner, M.; White, M. S.; Głowacki, E. D.; Sekitani, T.; Someya, T.; Sariciftci, N. S.; Bauer, S. Ultrathin and Lightweight Organic Solar Cells with High Flexibility. *Nat. Commun.* **2012**, *3*, 770.

(3) O'Connor, T. F.; Rajan, K. M.; Printz, A. D.; Lipomi, D. J. Toward Organic Electronics with Properties Inspired by Biological Tissue. *J. Mater. Chem. B* [Online early access]. DOI: 10.1039/C5TB00173K. Published Online: February 26, 2015.

(4) Savagatrup, S.; Printz, A. D.; O'Connor, T. F.; Zaretski, A. V.; Lipomi, D. J. Molecularly Stretchable Electronics. *Chem. Mater.* **2014**, *26*, 3028.

(5) Dou, L.; You, J.; Hong, Z.; Xu, Z.; Li, G.; Street, R. A.; Yang, Y. 25th Anniversary Article: A Decade of Organic/Polymeric Photovoltaic Research. *Adv. Mater.* **2013**, *25*, 6642.

(6) Li, H.; Tee, B. C.-K.; Giri, G.; Chung, J. W.; Lee, S. Y.; Bao, Z. High-Performance Transistors and Complementary Inverters Based on Solution-Grown Aligned Organic Single-Crystals. *Adv. Mater.* **2012**, *24*, 2588.

(7) Liu, T.; Troisi, A. What Makes Fullerene Acceptors Special as Electron Acceptors in Organic Solar Cells and How To Replace Them. *Adv. Mater.* **2013**, *25*, 1038.

(8) Burke, D. J.; Lipomi, D. J. Green Chemistry for Organic Solar Cells. *Energy Environ. Sci.* **2013**, *6*, 2053.

(9) Anctil, A.; Babbitt, C. W.; Raffaelle, R. P.; Landi, B. J. Material and Energy Intensity of Fullerene Production. *Environ. Sci. Technol.* **2011**, *45*, 2353.

(10) Savagatrup, S.; Makaram, A. S.; Burke, D. J.; Lipomi, D. J. Mechanical Properties of Conjugated Polymers and Polymer–Fullerene Composites as a Function of Molecular Structure. *Adv. Funct. Mater.* **2014**, *24*, 1169.

(11) Tahk, D.; Lee, H. H.; Khang, D.-Y. Elastic Moduli of Organic Electronic Materials by the Buckling Method. *Macromolecules* **2009**, *42*, 7079.

(12) Brand, V.; Bruner, C.; Dauskardt, R. H. Cohesion and Device Reliability in Organic Bulk Heterojunction Photovoltaic Cells. *Sol. Energy Mater. Sol. Cells* **2012**, *99*, 182.

(13) Dupont, S. R.; Voroshazi, E.; Heremans, P.; Dauskardt, R. H. Adhesion Properties of Inverted Polymer Solarcells: Processing and Film Structure Parameters. *Org. Electron.* **2013**, *14*, 1262.

(14) Jørgensen, M.; Norrman, K.; Gevorgyan, S. A.; Tromholt, T.; Andreasen, B.; Krebs, F. C. Stability of Polymer Solar Cells. *Adv. Mater.* **2012**, *24*, 580.

(15) Andersson, L. M.; Hsu, Y.-T.; Vandewal, K.; Sieval, A. B.; Andersson, M. R.; Inganäs, O. Mixed C60/C70 Based Fullerene Acceptors in Polymer Bulk-Heterojunction Solar Cells. *Org. Electron.* **2012**, *13*, 2856.

(16) Popescu, L. M. *Fullerene Based Organic Solar Cells*: University of Groningen: Groningen, The Netherlands, 2008.

(17) Kronholm, D. F.; Hummelen, J. C.; Sieval, A. B.; Van't Hof, P. U.S. Patent US 2013/8435716, 2013.

(18) Wienk, M. M.; Kroon, J. M.; Verhees, W. J. H.; Knol, J.; Hummelen, J. C.; van Hal, P. A.; Janssen, R. A. J. Efficient Methano[70]fullerene/MDMO-PPV Bulk Heterojunction Photovoltaic Cells. *Angew. Chem.* **2003**, *115*, 3493.

(19) Williams, E. D.; Ayres, R. U.; Heller, M. The 1.7 Kilogram Microchip: Energy and Material Use in the Production of Semiconductor Devices. *Environ. Sci. Technol.* **2002**, *36*, 5504.

(20) Anctil, A.; Babbitt, C. W.; Raffaelle, R. P.; Landi, B. J. Cumulative Energy Demand for Small Molecule and Polymer Photovoltaics. *Prog. Photovolt. Res. Appl.* **2013**, *21*, 1541.

(21) Awartani, O.; Lemanski, B. I.; Ro, H. W.; Richter, L. J.; DeLongchamp, D. M.; O'Connor, B. T. Correlating Stiffness, Ductility, and Morphology of Polymer/Fullerene Films for Solar Cell Applications. *Adv. Energy Mater.* **2013**, *3*, 399.

(22) O'Connor, B.; Chan, E. P.; Chan, C.; Conrad, B. R.; Richter, L. J.; Kline, R. J.; Heeney, M.; McCulloch, I.; Soles, C. L.; DeLongchamp, D. M. Correlations between Mechanical and Electrical Properties of Polythiophenes. *ACS Nano* **2010**, *4*, 7538.

(23) Dupont, S. R.; Oliver, M.; Krebs, F. C.; Dauskardt, R. H. Interlayer Adhesion in Roll-to-Roll Processed Flexible Inverted Polymer Solar Cells. *Sol. Energy Mater. Sol. Cells* **2012**, *97*, 171.

DOI: 10.1021/acs.chemmater.5b00638
Chem. Mater. 2015, 27, 3902–3911

(24) Liu, F.; Gu, Y.; Jung, J. W.; Jo, W. H.; Russell, T. P. On the Morphology of Polymer-Based Photovoltaics. *J. Polym. Sci., Part B: Polym. Phys.* **2012**, *50*, 1018.
(25) Lipomi, D.; Chong, H.; Vosgueritchian, M.; Mei, J.; Bao, Z. Toward Mechanically Robust and Intrinsically Stretchable Organic Solar Cells: Evolution of Photovoltaic Properties with Tensile Strain. *Sol. Energy Mater. Sol. Cells* **2012**, *107*, 355.
(26) Printz, A.; Savagatrup, S.; Burke, D.; Purdy, T.; Lipomi, D. Increased Elasticity of a Low-Bandgap Conjugated Copolymer by Random Segmentation for Mechanically Robust Solar Cells. *RSC Adv.* **2014**, *4*, 13635.
(27) Savagatrup, S.; Printz, A. D.; Rodriquez, D.; Lipomi, D. J. Best of Both Worlds: Conjugated Polymers Exhibiting Good Photovoltaic Behavior and High Tensile Elasticity. *Macromolecules* **2014**, *47*, 1981.
(28) Printz, A. D.; Savagatrup, S.; Rodriquez, D.; Lipomi, D. J. Role of Molecular Mixing on the Stiffness of Polymer/Fullerene Bulk Heterojunction Films. *Sol. Energy Mater. Sol. Cells* **2015**, *134*, 64.
(29) Brand, V.; Levi, K.; McGehee, M. D.; Dauskardt, R. H. Film Stresses and Electrode Buckling in Organic Solar Cells. *Sol. Energy Mater. Sol. Cells* **2012**, *103*, 80.
(30) Savagatrup, S.; Chan, E.; Renteria-Garcia, S. M.; Printz, A. D.; Zaretski, A. V.; O'Connor, T. F.; Rodriquez, D.; Valle, E.; Lipomi, D. J. Plasticization of PEDOT:PSS by Common Additives for Mechanically Robust Organic Solar Cells and Wearable Sensors. *Adv. Funct. Mater.* **2015**, *25*, 427.
(31) Stafford, C. M.; Harrison, C.; Beers, K. L.; Karim, A.; Amis, E. J.; VanLandingham, M. R.; Kim, H.-C.; Volksen, W.; Miller, R. D.; Simonyi, E. E. A Buckling-Based Metrology for Measuring the Elastic Moduli of Polymeric Thin Films. *Nat. Mater.* **2004**, *3*, 545.
(32) Stafford, C. M.; Guo, S.; Harrison, C.; Chiang, M. Y. M. Combinatorial and High-Throughput Measurements of the Modulus of Thin Polymer Films. *Rev. Sci. Instrum.* **2005**, *76*, 062207.
(33) Wilder, E. A.; Guo, S.; Lin-Gibson, S.; Fasolka, M. J.; Stafford, C. M. Measuring the Modulus of Soft Polymer Networks via a Buckling-Based Metrology. *Macromolecules* **2006**, *39*, 4138.
(34) Huang, D. M.; Mauger, S. A.; Friedrich, S.; George, S. J.; Dumitriu-LaGrange, D.; Yoon, S.; Moule, A. J. The Consequences of Interface Mixing on Organic Photovoltaic Device Characteristics. *Adv. Funct. Mater.* **2011**, *21*, 1657.
(35) Dupont, S. R.; Voroshazi, E.; Nordlund, D.; Vandewal, K.; Dauskardt, R. H. Controlling Interdiffusion, Interfacial Composition, and Adhesion in Polymer Solar Cells. *Adv. Mater. Interfaces* **2014**, 1400135.
(36) Verploegen, E.; Mondal, R.; Bettinger, C. J.; Sok, S.; Toney, M. F.; Bao, Z. Effects of Thermal Annealing upon the Morphology of Polymer−Fullerene Blends. *Adv. Funct. Mater.* **2010**, *20*, 3519.
(37) Miller, N. C.; Gysel, R.; Miller, C. E.; Verploegen, E.; Beiley, Z.; Heeney, M.; McCulloch, I.; Bao, Z.; Toney, M. F.; McGehee, M. D. The Phase Behavior of a Polymer−Fullerene Bulk Heterojunction System That Contains Bimolecular Crystals. *J. Polym. Sci., Part B: Polym. Phys.* **2011**, *49*, 499.
(38) Brady, M. M. A.; Su, G. G. M.; Chabinyc, M. M. L. Recent Progress in the Morphology of Bulk Heterojunction Photovoltaics. *Soft Matter* **2011**, *7*, 11065.
(39) Dang, M. T.; Hirsch, L.; Wantz, G. P3HT/PCBM, Best Seller in Polymer Photovoltaic Research. *Adv. Mater.* **2011**, *23*, 3597.
(40) Liao, S.-H.; Li, Y.-L.; Jen, T.-H.; Cheng, Y.-S.; Chen, S.-A. Multiple Functionalities of Polyfluorene Grafted with Metal Ion-Intercalated Crown Ether as an Electron Transport Layer for Bulk-Heterojunction Polymer Solar Cells: Optical Interference, Hole Blocking, Interfacial Dipole, and Electron Conduction. *J. Am. Chem. Soc.* **2012**, *134*, 14271.
(41) Krebs, F. C.; Espinosa, N.; Hösel, M.; Søndergaard, R. R.; Jørgensen, M. 25th Anniversary Article: Rise to Power—OPV-Based Solar Parks. *Adv. Mater.* **2014**, *26*, 29.
(42) Osedach, T. P.; Andrew, T. L.; Bulović, V. Effect of Synthetic Accessibility on the Commercial Viability of Organic Photovoltaics. *Energy Environ. Sci.* **2013**, *6*, 711.
(43) Kim, J. Y.; Frisbie, C. D. Correlation of Phase Behavior and Charge Transport in Conjugated Polymer/Fullerene Blends. *J. Phys. Chem. C* **2008**, *112*, 17726.
(44) Zhao, J.; Swinnen, A.; Van Assche, G.; Manca, J.; Vanderzande, D.; Van Mele, B. Phase Diagram of P3HT/PCBM Blends and Its Implication for the Stability of Morphology. *J. Phys. Chem. B* **2009**, *113*, 1587.
(45) Treat, N. D.; Brady, M. A.; Smith, G.; Toney, M. F.; Kramer, E. J.; Hawker, C. J.; Chabinyc, M. L. Interdiffusion of PCBM and P3HT Reveals Miscibility in a Photovoltaically Active Blend. *Adv. Energy Mater.* **2011**, *1*, 82.
(46) Treat, N. D.; Varotto, A.; Takacs, C. J.; Batara, N.; Al-Hashimi, M.; Heeney, M. J.; Heeger, A. J.; Wudl, F.; Hawker, C. J.; Chabinyc, M. L. Polymer−Fullerene Miscibility: A Metric for Screening New Materials for High-Performance Organic Solar Cells. *J. Am. Chem. Soc.* **2012**, *134*, 15869.
(47) Roehling, J. D.; Batenburg, K. J.; Swain, F. B.; Moulé, A. J.; Arslan, I. Three-Dimensional Concentration Mapping of Organic Blends. *Adv. Funct. Mater.* **2013**, *23*, 2115.
(48) Choi, S. H.; Liman, C. D.; Krämer, S.; Chabinyc, M. L.; Kramer, E. J. Crystalline Polymorphs of [6,6]-Phenyl-C61-Butyric Acid N-Butyl Ester (PCBNB). *J. Phys. Chem. B* **2012**, *116*, 13568.
(49) Zheng, L.; Liu, J.; Ding, Y.; Han, Y. Morphology Evolution and Structural Transformation of Solution-Processed Methanofullerene Thin Film under Thermal Annealing. *J. Phys. Chem. B* **2011**, *115*, 8071.
(50) Zheng, L.; Han, Y. Solvated Crystals Based on [6,6]-Phenyl-C61-Butyric Acid Methyl Ester (PCBM) with the Hexagonal Structure and Their Phase Transformation. *J. Phys. Chem. B* **2012**, *116*, 1598.
(51) Müller, C.; Ferenczi, T. A. M.; Campoy-Quiles, M.; Frost, J. M.; Bradley, D. D. C.; Smith, P.; Stingelin-Stutzmann, N.; Nelson, J. Binary Organic Photovoltaic Blends: A Simple Rationale for Optimum Compositions. *Adv. Mater.* **2008**, *20*, 3510.
(52) Treat, N. D.; Chabinyc, M. L. Phase Separation in Bulk Heterojunctions of Semiconducting Polymers and Fullerenes for Photovoltaics. *Annu. Rev. Phys. Chem.* **2014**, *65*, 59.
(53) Hopkinson, P. E.; Staniec, P. A.; Pearson, A. J.; Dunbar, A. D. F.; Wang, T.; Ryan, A. J.; Jones, R. A. L.; Lidzey, D. G.; Donald, A. M. A Phase Diagram of the P3HT/PCBM Organic Photovoltaic System: Implications for Device Processing and Performance. *Macromolecules* **2011**, *44*, 2908.
(54) Savagatrup, S.; Printz, A. D.; Wu, H.; Rajan, K. M.; Sawyer, E. J.; Zaretski, A. V.; Bettinger, C. J.; Lipomi, D. J. Viability of Stretchable Poly(3-heptylthiophene) (P3HpT) for Organic Solar Cells and Field-Effect Transistors. *Synth. Met.* **2015**, *203*, 208.
(55) Spano, F. C. Modeling Disorder in Polymer Aggregates: The Optical Spectroscopy of Regioregular Poly(3-hexylthiophene) Thin Films. *J. Chem. Phys.* **2005**, *122*, 234701.
(56) Turner, S. T.; Pingel, P.; Steyrleuthner, R.; Crossland, E. J. W.; Ludwigs, S.; Neher, D. Quantitative Analysis of Bulk Heterojunction Films Using Linear Absorption Spectroscopy and Solar Cell Performance. *Adv. Funct. Mater.* **2011**, *21*, 4640.
(57) Clark, J.; Chang, J.-F.; Spano, F. C.; Friend, R. H.; Silva, C. Determining Exciton Bandwidth and Film Microstructure in Polythiophene Films Using Linear Absorption Spectroscopy. *Appl. Phys. Lett.* **2009**, *94*, 163306.
(58) Zimmermann, E.; Ehrenreich, P.; Pfadler, T.; Dorman, J. A.; Weickert, J.; Schmidt-Mende, L. Erroneous Efficiency Reports Harm Organic Solar Cell Research. *Nat. Photonics* **2014**, *8*, 669.
(59) Louarn, G.; Trznadel, M. Raman Spectroscopic Studies of Regioregular Poly(3-alkylthiophenes). *J. Phys. Chem.* **1996**, *3654*, 12532.
(60) Pingel, P.; Zen, A.; Abellon, R. D.; Grozema, F. C.; Siebbeles, L. D. A.; Neher, D. Temperature-Resolved Local and Macroscopic Charge Carrier Transport in Thin P3HT Layers. *Adv. Funct. Mater.* **2010**, *20*, 2286.

DOI: 10.1021/acs.chemmater.5b00638
Chem. Mater. 2015, 27, 3902−3911